Natural Resources Research, Vol. 30, No. 3, June 2021 (© 2021)
https://doi.org/10.1007/s11053-021-09818-4

Original Paper

Geoelectrical Resistivity and Geological Characterization of Hydrostructures for Groundwater Resource Appraisal in the Obudu Plateau, Southeastern Nigeria

Ebong D. Ebong,[1,4] Augustine A. Abong,[2] Eric B. Ulem,[1] and Loveth A. Ebong[3]

Received 10 July 2020; accepted 16 January 2021
Published online: 3 February 2021

Electrical resistivity tomography (ERT) and vertical electrical sounding (VES) techniques were employed to assess the hydrogeological structures and groundwater potential of the Obudu Basement Complex. The Wenner electrode configuration was used to acquire the ERT data along 4 profiles, while the Schlumberger configuration was employed in the VES investigation, where 30 locations were occupied during the data acquisition campaign. Results show that rock distribution is predominantly the granite gneiss series that are considerably weathered in several locations especially within the western portion of the study area. Three potential hydrogeological scenarios were identified from three of the ERT profiles. These include the regolith-, doleritic- and kaolin-induced groundwater conduits. Within the central segment of the study area, transtensional stress regimes traceable to the neo-Proterozoic syn-orogenic event were observed to have resulted in the establishment of some regional fault systems. Over time, several episodes of minor tectonic events have resulted in cataclastic deformation of the gneissic rocks, creating pathways for groundwater circulation. Additionally, it was observed that dolerite intrusion in some locations cataclastically deformed the host rock resulting in syn-emplacement fractures that can create pathways for groundwater to flow. Saprolite units and locations within major fault lines were inferred to have moderate to good groundwater potential due to their large width and the presence of multiple interconnected fractures as inferred from the pseudo-sections and lineament map. More so, streams and rivers within these areas can infiltrate through the pathways created by the faults, hence increasing groundwater circulation within the conduits.

KEY WORDS: Electrical resistivity, Fracture, Fault, Lineament, Hard rock, Obudu complex.

INTRODUCTION

Water remains the world's most widely distributed resources, which exist as either surface water or groundwater. The availability of water has always played a significant role in determining settlement pattern and quality of life of inhabitants in a defined area (Fang and Jawitz 2019). Studies show that large amounts of water abound on earth, but its distribution makes the resources scarce in some

[1]Applied Geophysics Programme, Physics Department, University of Calabar, PMB 1115, Calabar, Cross River State, Nigeria.
[2]Department of Physics, Cross River University of Technology, Calabar, Cross River State, Nigeria.
[3]Department of Computer Engineering, University of Calabar, PMB 1115, Calabar, Cross River State, Nigeria.
[4]To whom correspondence should be addressed; e-mail: dickebong@yahoo.co.uk, ebongdickson@unical.edu.ng

areas (O'Connor et al. 2008; Orlović and Krajnović 2015).

Groundwater conduits are defined by their vertical and lateral continuities, nature of connectivity of pores and ability to transmit water, all of which determine yield (Runkel et al. 2006). Groundwater movement within such portions of the subsurface is influenced by hydrostatic head. However, this assumption may not always hold, especially in basement terrains. In basement complexes like the Precambrian Crystalline Basement Complex, the availability and characteristics of groundwater conduits are greatly influenced by regional geological history and other environmental factors such as amount of rainfall (Titus et al. 2009).

About 40% of land occupied by over 220 million rural dwellers in sub-Saharan Africa is composed of crystalline basement rocks (MacDonald and Davies 2000). Studies have shown that groundwater yield within this area is generally marginal to poor, due to inadequate water storage capacities of the rocks and poor recharge conditions (Wright 1992; Okwueze 1996). Crystalline rock aquifers that are basically fractured igneous and metamorphic rocks have been reported to possess negligible matrix porosity and permeability (Gustafson and Krásný 1994). These fractures that are variable in nature, depending on their frequency of distribution in space and interconnectivity, are products of intense tectonic activities (Titus et al. 2009; Singhal and Gupta 1999). The crystalline basement aquifers are fractured bedrocks that occur occasionally along lineaments and correspond to the surface drainage pattern (Adams 2009) and the overlying weathered basement materials, i.e., regoliths (Chilton and Foster 1995). Inasmuch as fractures are well known to be groundwater exploration targets in hard rock terrains, it is required that fracture sets are interconnected to form a network of fractures to have adequate yield (Satpathy and Kanungo 1976; Berkowitz and Balberg 1993; Ebong et al. 2014; Liu et al. 2016).

Besides fractured basement aquifers, regolith aquifers occur in areas where relatively thick weathered basement rocks that can meet the requirements of groundwater storage and abstraction exist. Regoliths are formed due to chemical weathering of crystalline basement rocks. The progressive chemical degradation process results in subhorizontal decompression of crystalline bedrock (Wright 1992). The development of regolith aquifers depends on the nature of basement rock, i.e., age, structure and lithology. Additionally, regolith aquifers are influenced by relief and climatic conditions (Mao et al. 2018).

The inhabitants of Obudu, Obanliku and part of Boki in Cross River State, Nigeria, which lie within the Obudu Basement Complex (i.e., part of the Eastern Nigerian Basement Complex), are plagued with severe water scarcity challenges. In a bid to cushion the adverse effects of their problem, the rural dwellers have subscribed to hand-dug wells and ephemeral springs for their domestic and drinking water needs. The water needs for all purpose by the rural dwellers in the area necessitated our study. The peculiar nature of water scarcity in basement terrains such as the Obudu complex has led geoscientists to develop several techniques that can ease the exploration and exploitation of groundwater resources.

The geophysical techniques usually employed in groundwater exploration include electrical resistivity, seismic refraction and electromagnetic methods. Electrical resistivity methods have enjoyed enormous patronage in locating shallow subsurface fractures (Robert et al. 2011; Ebong et al. 2014; Almadani et al. 2019) and faults (Suzuki et al. 2000; Fazzito et al. 2009), which are groundwater exploration targets in hard rock environments (Titus et al. 2009; Singhal and Gupta 1999). These non-invasive methods combine speed, accuracy and cost-effectiveness in defining the depth to groundwater, fracture zones and other bedrock discontinuities, and have over the years been veritable tools for groundwater exploration (Akpan et al. 2013, 2015a; Ebong et al. 2014; Ejiogu et al. 2019; Ekwok et al. 2020). Electrical methods are known to provide certain degree of variation in electrical properties of rocks that can help in delineating inter-aquifer relationship of multi-aquifer systems in complex geological settings (Inoubli et al. 2006; Samsudin et al. 2008; Ndubueze et al. 2019).

Wide ranges of hydrological and hydrogeological challenges like groundwater flow modeling, groundwater prediction, groundwater characterization, groundwater protection and remediation have been solved using coupled geophysical and hydrogeological assessments (Wilkinson et al. 2010; Attwa et al. 2014; Akpan et al. 2015b, 2018; Ebong et al. 2017; Peinado-Guevara et al. 2017). Geospatial information of groundwater structures derived from electrical resistivity tomography (ERT) and vertical electrical sounding (VES) have been used to investigate groundwater conditions (Obianwu et al. 2015;

George et al. 2015), groundwater-induced landslide sites (Akpan et al. 2016) and geological and structural characterization of basins (Gélis et al. 2010; Akpan et al. 2018). ERT can also provide useful hydrogeological information in highly weathered and fractured rocks (Robert et al. 2011). The dependence of geological materials on electrical properties forms the basis for its continuous usage in hydrogeological investigations.

This study was aimed at delineating geological structures and groundwater conduits in hard rock terrains by exploiting the reliability of joint electrical resistivity techniques in delineating fractures and weathered basement rocks.

SITE DESCRIPTION AND GEOLOGY

The study area covers about 1465 km^2 within the northern part of Cross River State and falls within Obudu and Obanliku. It lies between longitudes 8° 40′ and 9° 30′ E and latitudes 6° 15′ and 6° 45′ N (Fig. 1). The study area is bounded by parts of the Benue and Taraba States to the north and to the west, Ogoja. It shares its eastern and southern boundaries with Boki and the Republic of Cameroon, respectively. The area has a tropical climate with distinct seasons: wet and dry seasons. The wet season begins in April and ends in September, while the dry season starts from October and ends in March. The temperature during the dry season ranges between 26 and 32 °C and drops in the rainy season to about 4 °C at the peak of the Obudu Plateau with elevation of ~ 1716 m above mean sea level. Annual rainfall ranges between 200 and 250 cm and can soar to ~ 420 cm at the peak of the Plateau. The rise in rainfall around the peak of the Plateau is due to the barrier created by the Sankwala Mountains, which forces the moisture laden Atlantic Air Mass that blow across the region upward resulting in rapid cooling and condensation. Relative humidity is between 40 and 80% around the Plateau (Edet and Okereke 2005). The area is predominantly hilly, and elevation varies from ~ 150 to > 1800 m above mean sea level and extends into the Republic of Cameroon as part of the Bamenda Plateau. The rugged hilly terrain is occasionally interrupted by networks of deep interlocking gorges which are potential targets for groundwater exploration.

Geologically, the area is composed of Precambrian rocks (Fig. 1), which are categorized into two groups, i.e., the Migmatitic Gneiss Complex (MGC) and the Pan African Older Granites (PAOG). The MGC includes relics of ancient metasedimentary sequence, migmatite unit largely composed of paleosomatic banded paragneisses, banded ironstones, ferruginous quartzites mixed with younger quartzofeldspatic granites and aplites and the gneisses occur as granitic, hornblende and augen gneisses. The PAOG is composed of undifferentiated granites, migmatites, charnockites, granulites, amphibolites and schists, which have been intruded by rocks of acidic, intermediate, basic and ultra-basic compositions (Ukwang et al. 2003). Rocks of the MGC are presumably the oldest and most predominant in the Nigerian Basement Complex (Odeyemi 1981). The Precambrian suite of plutonic gneissose granite that constitute coarse grained phyritic/porphyritic granites, fine-grained granites granodiorites and quartzdiorites occur as massive batholiths in many locations within the Basement complex (Ekwueme 1990). The banded gneiss, which is in high abundance within the area, occurs as massive rocks and consist of alternating bands of felsic minerals, notably plagioclase feldspar, quartz and dark colored rocks like biotite and hornblende (Ekwueme 2003).

Other rocks in the Obudu Plateau include garnet-hornblende gneiss, biotite-garnet schist and garnet-sillimanite gneiss, which are intruded by pegmatite (Ekwueme 1994). The linear and dilational orientations of these rocks indicate forceful emplacement into pre-existing zones. Contrasts in the thermal states of the host rocks and pegmatites are indicated by the fine-grained nature of the contact zone. These alterations in rock composition are due to fractional and progressive reactions between remnant rock crystals and incoming fluid. The ultramafic schists in the Sankwala area, which have attained high grade metamorphism (i.e., granulite facies), are highly deformed and intensely weathered (Ekwueme 1990). Folding of schist is widespread in some areas. The schistosity of rock is strong and trend in the dominant N–S to NE–SW directions. Around Sankwala Hills, the garnet hornblende gneissic rock have been subjected to intense folding and shearing and are sometimes wrapped around xenoliths. At Busangfong area, folding and refolding of foliation are sporadic, and gneissic rocks are inter-banded on a megascopic scale with quartzite veins (Edem et al. 2016). At Bishiri, massive quartz veins that extend beyond 100 m with multiple fractures exist (Oden et al. 2012). Rounded boulders of dolerites occur as minor

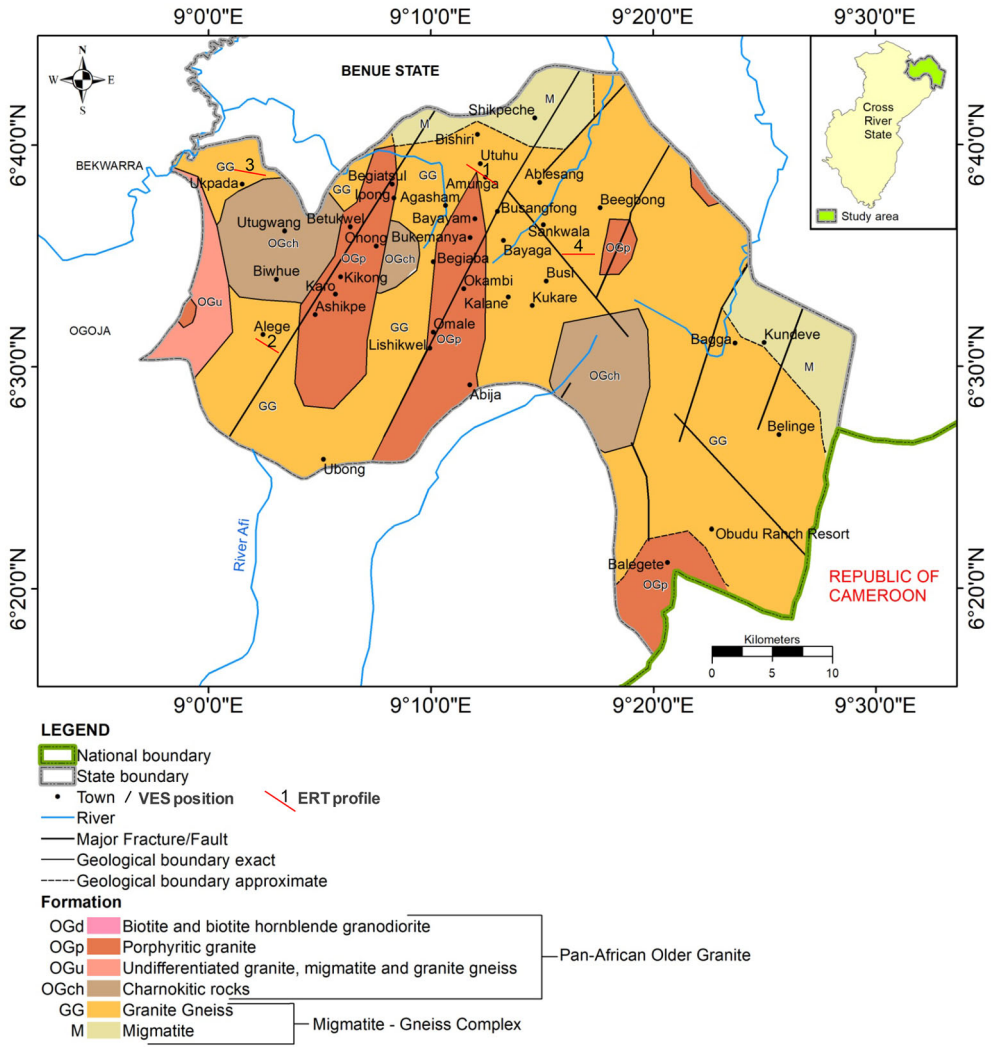

Figure 1. Geologic map of study area showing locations of vertical electrical soundings (small dots) and electrical resistivity tomography profiles (red lines).

components in some parts of the area. Dolerite dykes trending N–S cut amphibolites, which are banded and have sharp contact due to brittle deformation. Boulders of garnet gneisses and charnockites that are weakly foliated are abundant around Bagga.

METHODS

Geoelectrical Resistivity Data Acquisition

In this study, ERT surveys were performed along four profiles to generate 2-D images of the vertical and lateral distributions of rocks and structures. The Lund imaging signal averaging system (SAS) 4000 consisting four input channels, clip-on battery, an external battery connector, cable with 64 electrode take-outs, an ES10-64 switching unit, manufactured by ABEM Instruments, Sweden, was used during the ERT data acquisition. The ERT profiles were located in areas where topographic variations were low, i.e., $\leq$ 0.6 m (Scapozza and Laigre 2014). The minimum and maximum number of stacks was set at 1 and 4 stacks, respectively. Although the maximum stacks was 4, during data acquisition, where the root mean square (RMS) error between measurements were less than the pre-

fixed error limit of 1.0%, the measurement cycles automatically terminated and displayed the reading. The total cycle time was set at 2 s, which corresponded with acquisition delay of 0.1 s and acquisition time of 0.2 s. The mode was set at 'Auto' and the output current injected into the ground varied between 100 and 200 mA. The Wenner electrode configuration, with minimum electrode separation of 5 m and maximum separation of 35 m for profiles 1, 3 and 4 and 50 m for profile 2, was used during the ERT investigation. The profile lines were located perpendicularly across major geological structures in order to capture subsurface heterogeneities within the area. Data acquisition was limited by prevailing field conditions such as settlement styles, steeply sloped hills and general restrictions by the populace. Electrical contact with the ground was checked and was good (i.e., contact resistances varied from 190 to 250 Ω) (Uhlemann et al. 2018).

Due to the ill-posed nature of inverse resistivity problems (LaBrecque et al. 1996), it is important to make good estimates of the true data error to avoid either over- or under-estimation during interpretation of the inverted models. Both estimation problems can result in the creation of artifacts that are nonexistent within the subsurface. Hence, the quality of the acquired data was checked using the reciprocal error technique. The reciprocal error technique is a repeatability test that provides precision in measurements and not accuracy (Robert et al. 2011); 5% was fixed as the maximum acceptable value of reciprocal error. This was realized by interchanging the current and potential electrodes. The data acquired were modeled using RES2DINV code. The blocky inversion technique, which utilizes the finite difference method in the generation of inverted apparent resistivity 2-D sections, was used. Due to the non-uniqueness of inversion models, the quasi-Newtonian optimization code was used to stabilize the inversion process, and after few iterations the difference between observed and theoretical data was represented by means of the absolute error (Sasaki 1992; Loke and Barker 1996; Loke 2004). Rock exposures along road cuts, mine walls and few available lithologic logs from drilled tube wells were used as constraints during the interpretation phase.

In this study, VES data were acquired not just to complement the ERT results and/or reduce the non-uniqueness problems associated with geophysical data, but also to extend the subsurface image provided by the ERT to give deeper rock electrical resistivity information. The Schlumberger electrode configuration that can be used to assess resistivity distributions at shallower and deeper depths was employed (Yadav and Singh 2007; Akpan et al. 2018). Over 30 randomly sited VES points, spread across the entire area that could be accessed (Fig. 1), were acquired using the IGIS signal enhancement resistivity meter (model SSP-MP-ATS), India. Although the resistivity meter has the capacity to average up to 32 cycles of values, the measurement cycles were truncated after 4 stacks, if the reading on the liquid crystal display correlated well, having standard deviation $< 5\%$. Half of the current electrode separation (AB/2) ranged between 1 and 250 m while that of the potential electrode (MN/2) varied from 0.25 to 10 m. The variation in the potential electrode separation was meant to enhance the input signal strength. Upon completion of the field surveys, the VES data were modeled using the RESIST code developed by Vander Velpen and Sporry (1993). Lithologic data from nearby wells, road cuts and artisanal mine pits were used to constrain the 1-D inverted models. After a couple of iterations, acceptable difference between the observed field data and theoretical data were represented by means of RMS error which was generally less than 5% (Fig. 2).

Lineament Extraction

Lineaments were extracted manually from a shaded-relief map produced from a digital elevation model (DEM) acquired by Shuttle Radar Topographic Mission (SRTM), developed by the Jet Propulsion Laboratory of the National Aeronautics and Space Administration (NASA). The SRTM-DEM, which can be downloaded from https://glovis.usgs.gov, has spatial resolution of 3 arc-seconds (90 m). The DEM format was Geo-Tiff and the coordinate system WGS 84/UTM Zone 32° N. The DEM represents actual relief projection based on tonal variations due to the direction of sunlight. This characteristic feature of the DEM provides a simple and effective way of lineament and fault extraction, because the data are readily available (Ganas et al. 2005). Non-geological structures such as roads were identified using Landsat-8 image and were eliminated from the shaded-relief map (Das and Pardeshi 2018).

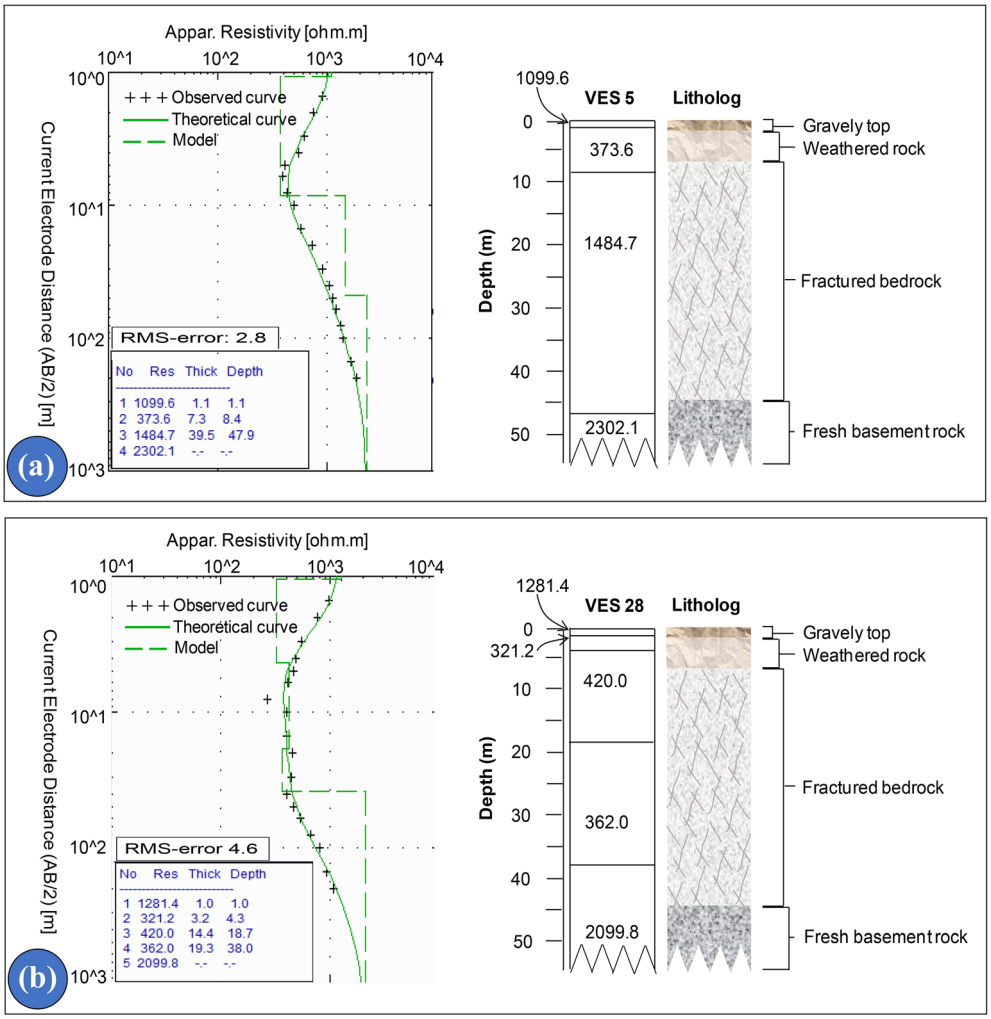

Figure 2.. 1-D inverted electrical resistivity model showing correlation of geoelectrical layer parameters (i.e., thickness and resistivity) and litholog from a nearby borehole. (**a**) Geoelectrical and litholog correlations at Karo area (VES 5). (**b**) Geoelectrical correlation using litholog from Karo area, which is closest to the geoelectrical sounding point (VES 28).

RESULTS AND DISCUSSION

Hydrostructural and Mineralized Zone Characterizations

The result of the VES investigations that show 1-D electrical resistivity and thickness of geoelectrical layers is represented in Table 1. In addition, the inversion of ERT data is represented as 2-D pseudo-sections in Figures 3, 4 and 5. ERT profile 1 (Fig. 3), oriented NW–SE perpendicular to the strike of the dominant geological structure within the area, was investigated in the vicinity of an extensive fault line (Fig. 1). The pseudo-section shows relatively high resistivity $> 800\ \Omega$ m from the beginning of the profile to ~ 65 m along the profile and extends vertically to depths of ~ 12.5 m. The highly resistive rock that is predominant in the area with exposures at several locations is granitic gneiss and constitutes part of the granite gneiss mass of the Pan-African Basement Complex. These granite gneisses are products of high grade metamorphism that occurred during Proterozoic. Deformation of the Precambrian basement rock opened up pathways for intrusions that later filled some fractures and faults within the area. The lateral continuity of the relatively high resistive rock was truncated by lowly resistive post-orogenic intrusive rock with

Table 1. Geoelectrical resistivity layer parameters from VES data

Location	VES points	Resistivity (Ω m)						Thickness (m)				
		ρ_1	ρ_2	ρ_3	ρ_4	ρ_5	ρ_6	h_1	h_2	h_3	h_4	h_5
Ukpada	1	34.0	130.0	225.2	1240.6	–	–	2.9	6.7	10.2	–	–
Udigie	2	884.6	483.3	156.4	2295.3	–	–	1.9	8.4	16.0	–	–
Shikpeche	3	214.6	62.2	277.3	681.4	–	–	1.1	7.0	28.1	–	–
Shikpeche2	4	161.2	51.3	155.4	3632.6	–	–	1.4	6.5	35.5	–	–
Karo	5	1073.5	273.1	1547.0	1127.3	4546.2	–	1.3	4.3	34.2	50.1	–
Biuhwe	6	1381.0	353.3	1422.8	1468.8	–	–	2.4	11.4	31.0	–	–
Alege	7	149.8	31.0	470.1	3139.0	5927.0	–	1.1	6.5	8.5	10.8	–
Ashikpe	8	430.6	3020.0	270.0	943.1	1684.3	–	0.9	4.1	17.3	36.3	–
Okambi	9	680.3	230.1	958.4	1427.5	422.1	702.2	3.2	9.5	12.6	16.8	22.0
Okambi2	10	685.5	236.4	1558.1	1911.4	–	–	2.2	7.5	14.0	26.8	–
Okordem 1	11	897.5	96.0	910.5	3344.8	–	–	1.0	5.9	46.8	–	–
Okordem 2	12	592.7	80.5	275.5	1253.0	–	–	2.5	5.6	63.6	–	–
Ohung	13	1493.1	144.7	1624.2	1348.8	–	–	5.9	11.0	27.3	–	–
Beegbong1	14	232.0	137.8	30.0	111.1	438.5	–	0.6	2.6	15.7	25.9	–
Beegbong2	15	157.1	14.1	100.0	1535.0	–	–	3.3	6.6	36.5	–	–
Ablesang	16	715.6	44.4	150.5	1508.7	–	–	0.7	12.8	27.5	–	–
Amunga	17	181.2	567.8	143.0	2401.5	–	–	0.3	4.6	35.4	–	–
Bayayam	18	215.3	58.0	208.1	1146.2	–	–	1.8	12.6	45.9	–	–
Begiatsul	19	105.3	805.9	252.0	2278.6	–	–	0.2	8.5	41.3	–	–
Bukemanya	20	327.4	37.3	272.7	1802.7	–	–	2.2	4.3	35.1	–	–
Kundeve	21	336.9	889.7	495.3	3329.3	–	–	0.2	13.8	24.3	–	–
Agasham	22	147.3	38.6	814.1	9427.5	–	–	1.3	4.8	49.5	–	–
Utugwang	23	141.4	181.6	2401.1	89.4	3186.0	–	2.0	7.8	10.8	17.2	–
Kalena	24	397.2	40.8	6573.0	9752.0	–	–	1.2	5.9	25.3	–	–
Kukare	25	135.9	297.1	558.6	4214.0	–	–	2.3	11.0	13.5	–	–
Sankwala	26	757.5	390.1	886.8	204.1	9457.9	–	1.5	10.5	9.1	32.9	–
Lishikwel	27	40.3	115.2	195.8	3202.0	–	–	0.3	5.2	46.0	–	–
Kikong	28	1281.4	321.2	420.0	362.0	2099.8	–	1.0	4.3	18.7	38.0	–
belinge	29	285.2	3124.2	1005.6	5102.0	6527.0	–	0.2	1.3	11.6	105.0	–
Ubong	30	1112.5	3798.7	470.9	987.3	3521.0	–	1.0	2.0	4.3	95.0	–

apparent resistivity of $\sim$ 500 Ω m. These intrusives, which are mostly doleritic and granodioritic, are known to occur as dykes and can be traced to the late syn-tectonic and post-tectonic episodes during the neo- and post-Proterozoic orogenies, respectively. An intrusive that occurred within the vicinity of a transtensional strike-slip fault led to the expansion of the fault zone to $\sim$ 10 to 15 m in width. The relatively low apparent resistivity values ($\sim$ 500 Ω m) observed within the vicinity of the dyke structure indicates that the pre-deformed rocks have been crushed cataclastically and weathered due to the interaction of the formation with percolating water. The granite gneiss rock continued laterally from $\sim$ 75 m along the profile to the end of the profile. The relatively high resistive granite gneiss shield mass is underlain by a lowly resistive rock suspected to be a sill. The sill structure is probably a member of the granite series that has been intensely weathered due to dissolution from percolating water leaching through the flanks of the intrusive rock. Fluid pressure from percolating water and pressure from the overlying rock strata may have increased the weathering and fracturing processes, thereby increasing the permeability and influx of water through to the sill. The sill layer has resistivity in the range of 200–400 Ω m and constitutes the aquifer conduit within the area. Such localized high fracture density zones are known to transmute into cataclasite formation, which provides bulk of the aquifer conduits in hard rock terrains. The VES data acquired along the eastern part of the profile to validate the ERT result and extend the depth of investigation also show a distinctive lowly resistive rock ($<$ 300 Ω m) overlain by the granite gneiss shield. This layer that was inferred to be an extension of the sill structure continued vertically to 40 m with thickness of $\sim$ 15 m. The sill structure is

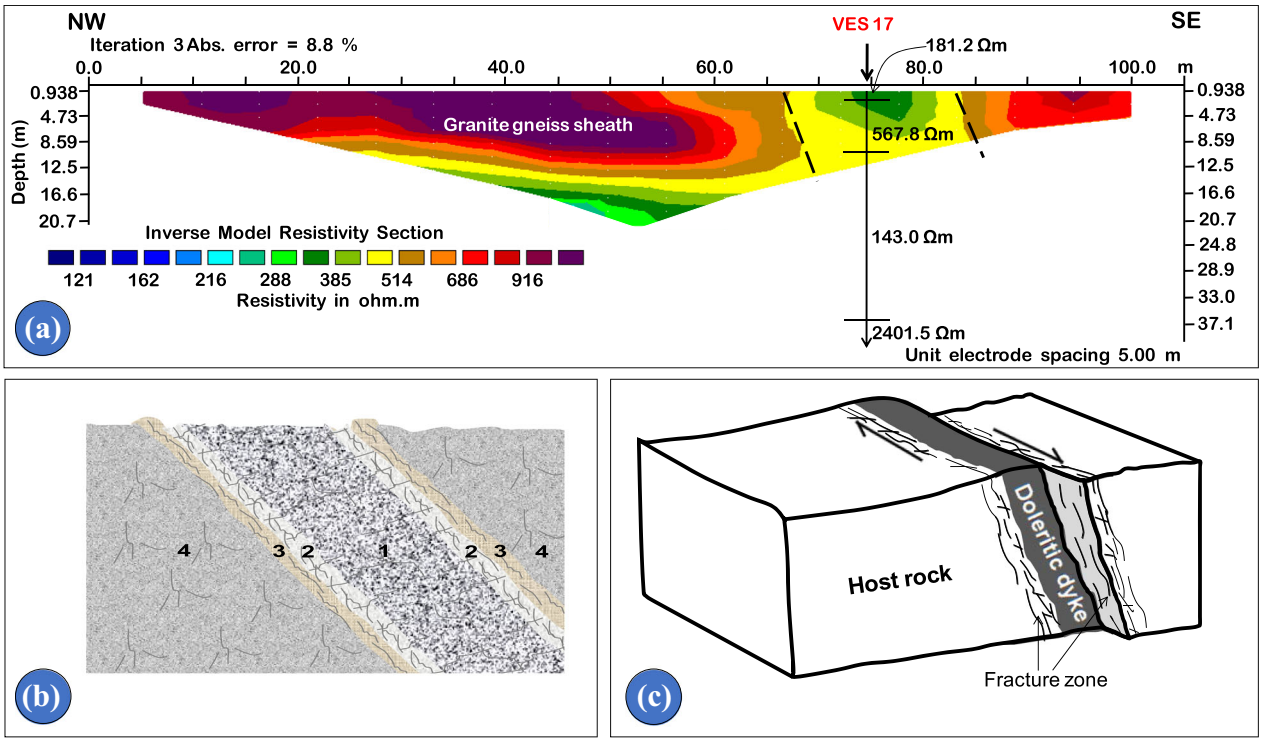

Figure 3. (**a**) 2-D inverted electrical resistivity image of the shallow subsurface within Amunga area correlated at about 70 m along the profile with a depth sounding result. (**b**) 2-D hypothetical model of a dolerite dyke system. (**c**) 3-D structural model showing fracture zones along a strike-slip fault filled with dolerite intrusion.

underlain by a highly resistive rock interpreted to be the country rock (i.e., granite gneiss) with $\rho_a \geq 2400$ Ω m.

The 2-D resistivity model shown in Figure 4 (i.e., profile 2) was investigated close to a kaolin mine pit at Alege. It was observed that the profile, which was laid in an E–W direction, intersected a dip-slip reverse fault. The beginning of the profile, which rests on the hanging wall, extends to ∼ 45 m along the profile and shows geoelectrical layer resistivity ranging from ∼ 100 to ∼ 700 Ω m with thickness of ∼ 7 m. The hanging wall, which was interpreted to be granite gneissic in composition, has been highly weathered due to its closeness to the surface. Its weathered counterparts are well exposed within the area. Slightly beneath the hanging wall is a relatively low resistive (< 200 Ω m) rock, interpreted to be water-wet granite gneiss that extends beyond 14 m depth. This zone is a potential groundwater conduit within the area. Across the fault zone is a lowly resistive layer of clay (i.e., kaolinite) with resistivity < 40 Ω m and extends laterally to ∼ 122 m along the profile with thickness of ∼ 10 m. The occurrence of kaolin may be traced to the thermo-tectonic episode, which released hydrothermal fluid that altered the chemical properties of the igneous rocks (i.e., hypogene process) within the vicinity of the fault. The migrating fluid up-dip found a near-surface conduit where it interacted with granitic rock to form kaolin and its equivalent clay minerals. Reverse faults of this nature expose metamorphic rocks such as gneisses to the surface as observed in some outcrops scattered around the vicinity of ERT profile. Some few meters away from the profile is a local mine pit ∼ 7 m in diameter, and VES data were also acquired close to the mine pit to validate the ERT result (Fig. 4c). Beneath the kaolin deposit is the weathered part of the footwall, composed of saprolite/saprock ∼ 6 m thick, which is the metamorphosed component of the granitoid substratum ($\rho_a \geq 3000\,\Omega$ m). The orientation of the fault is an indication that the hanging wall can provide better groundwater targets as the fault plane can induce fracture network that can transmit fluid. The development of such fracture network and grain scale brittle deformation can result in increased permeability as well as induce the influx of fluid into the fault zone. The top of the

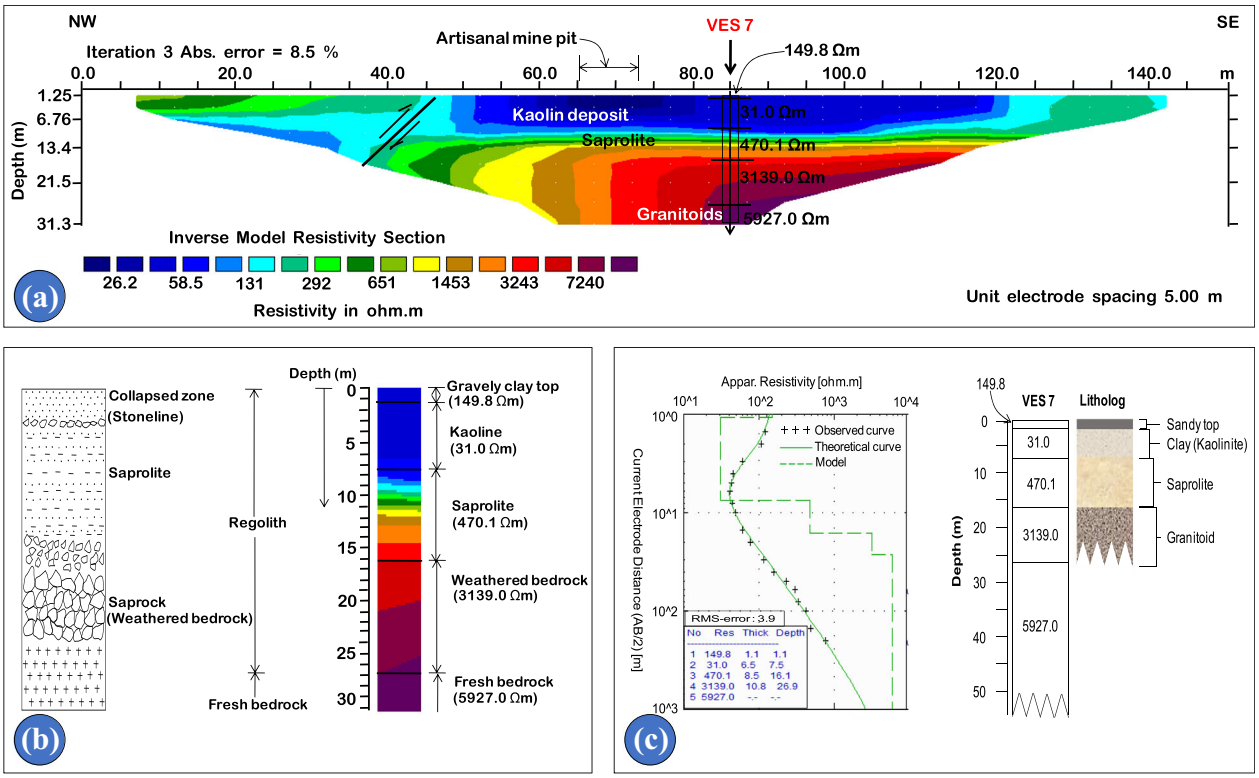

Figure 4. (**a**) 2-D inverted electrical resistivity image of the shallow subsurface within Alege area correlated with a VES result at 85 m along the profile. (**b**) 1-D inverted electrical resistivity model correlated with rock profile of the Oban Massif adapted from Edet and Okereke (1997). (**c**) Fitted observed field curve and theoretical curve with RMS error of 3.9% and geoelectrical layer parameters correlated with subsurface slice (litholog) from a nearby (~ 5 m away from the ERT line) artisanal mine pit.

footwall, which constitutes the weathered rock formation, overlies the kaolin deposit and extends vertically through ~ 7 m depth toward the granitoid substratum. This thick saprolite and saprock serves as groundwater exploration target. The static water level in the mine pit was ~ 2 m, which is a strong indication of groundwater potential of the weathered layer and saprolite/saprock formation (i.e., regolith). The conceptual model of groundwater resource potential and kaolinization is shown in Figure 6.

Figure 5 shows the ERT profile acquired around Ukpada area. The top of the inverted 2-D resistivity model shows a layer of weathered rock 12 m thick with resistivity ranging < 43.4 to 185.3 Ω m. The VES measurements, which were carried out with smaller inter-electrode spacing (i.e., AB of 2 to 10 m) and thereafter gradually increased until it reached ~ 600 m, were used to distinguish the humus top soil with resistivity of 34.0 Ω m (~ 3 m thick), and the sandy silt layer with resistivity of 130.0 Ω m (~ 8 m thick) of the regolith layer correlated strongly with the ERT data. The weathered rock observed to be gravelly-sandy-clay was interpreted as regolith resulting from fragmentation of migmatitic rocks that are dominant in the area. The regolith layer is underlain by fragments of weathered migmatitic rocks (i.e., saprock) with relatively high resistivity ranging from < 220.0 to ~ 400.0 Ω m and ~ 7 m thick. The regolith and saprock in this area constitute potential targets of groundwater exploitation.

Edet and Okereke (2005) reported that areas of thick regolith layer within the Obudu Basement Complex are devoid of intense fracturing activities; hence, lineament density in such areas is usually low. In such situations, regolith formation may not be connected to fracturing but intense chemical degradation due to the complex interaction of leached acidic water from precipitation and mineral grains of the bedrock. Other factors include temperature alternation during wet and dry seasons, strong oxidation and subdued topography (Levinson 1980; Edet and Okereke 2005). Hydrogeological explo-

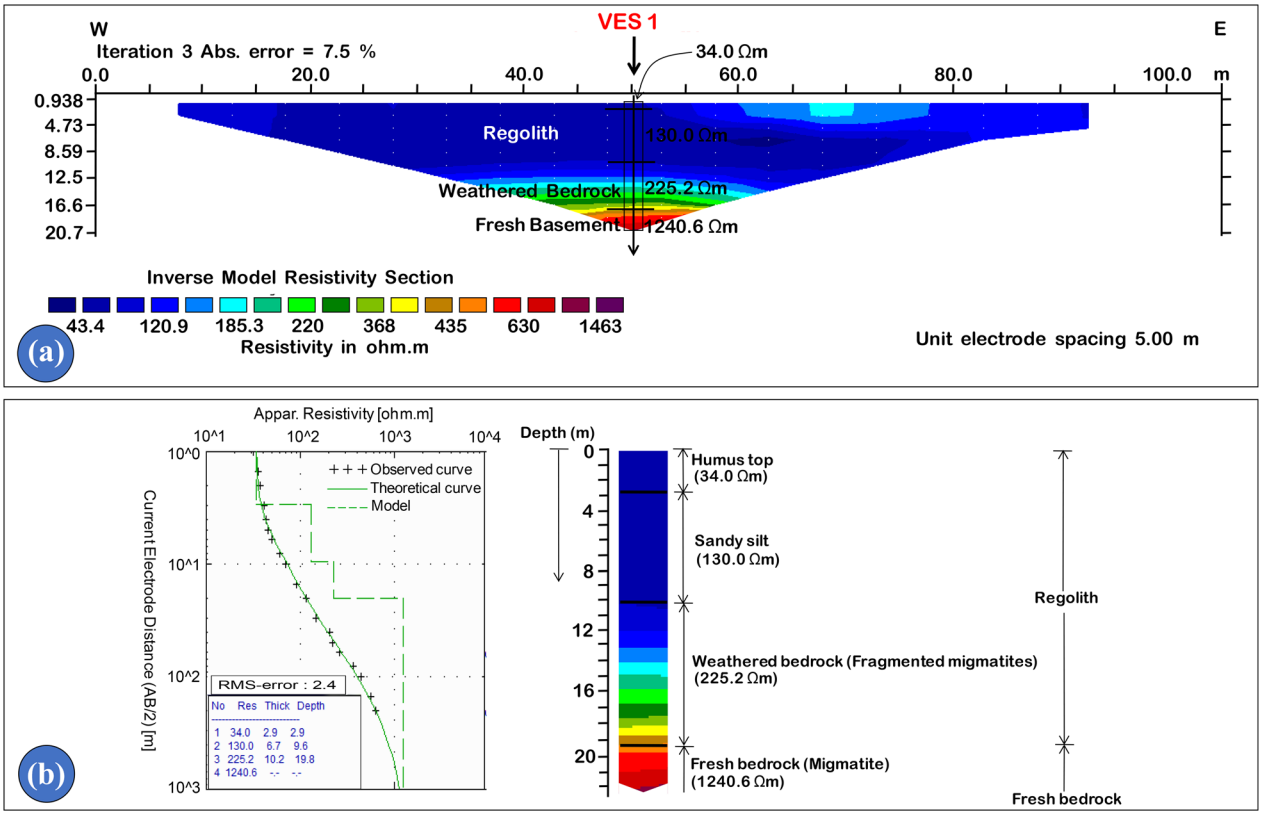

Figure 5. (**a**) 2-D inverted electrical resistivity image of the shallow subsurface in Ukpada area correlated with a vertical electrical sounding result at 85 m along the profile. (**b**) Fitted observed field curve and theoretical curve with RMS error of 2.4% and geoelectrical layer parameters correlated with rock profile of the Oban Massif adapted from Edet and Okereke (1997).

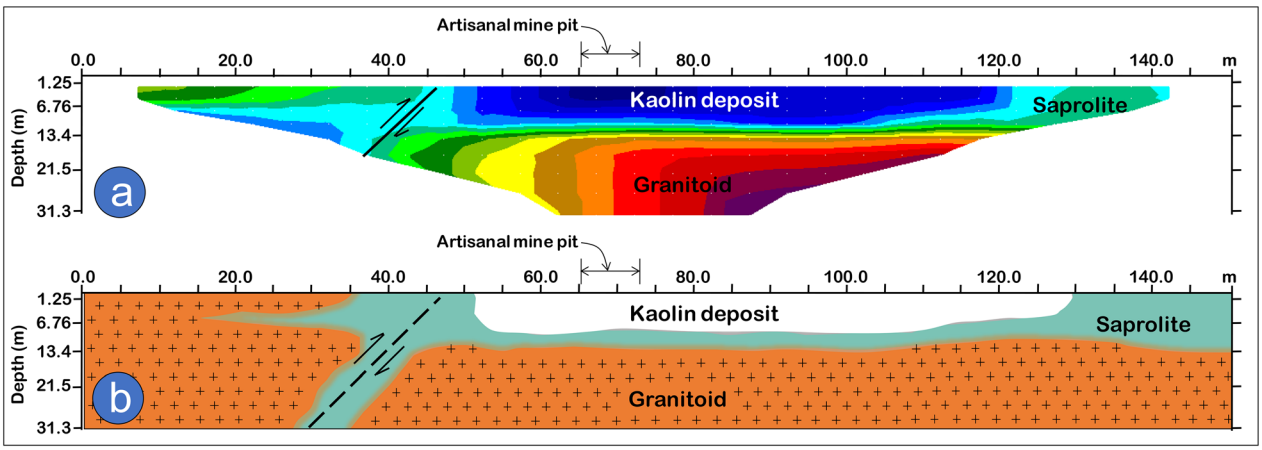

Figure 6. (**a**) 2-D inverted electrical resistivity image of the shallow subsurface in Alege area. (**b**) Conceptual model of kaolinization showing structural discontinuity, which creates pathway for groundwater mobilization and transmission through the saprolite layer.

ration of productive borehole sites within this area should target areas with thick regolith layer instead of trying to locate fractures and faults. The weathered migmatitic rocks are underlain by fresh impermeable migmatitic substratum with resistivity > 1200.0 Ω m.

Groundwater Conduit Delineation

The complex geological conditions experienced within the Obudu Plateau are to the advantage of hydrogeologist, as these can increase their chances of success during groundwater exploitation campaigns. Three potential hydrogeological scenarios were identified from four of the ERT investigations in the area. The first is the zone of regolith aquifer, which is predominant within the western portion of the study area. This area is devoid of intense fracturing and its lineament density is low. Edet and Okereke (2005) reported that areas with such sparse lineament systems or large fracture spacing are likely areas of thick regolith layers within the hard rock environment. The ERT and VES investigations within the western flank of the study area revealed regolith thickness ranging from $\sim$ 12 to 20 m and electrical resistivity values of 20–150 Ω m. The range of regolith thickness is relatively adequate for groundwater circulation within the western part (i.e., around Shikpeche Ukpada, Otugwang and Biwhue) of the study area. The groundwater potential within this area is moderate to poor because the regolith layer is slightly greater than 10 m, although it may extend beyond 15 m due to the influence of topographic gradient. Water wells in this area may dry up during the dry season when the major source of recharge (i.e., precipitation) ceases.

Areas within dolerite intrusions were also delineated as possible targets for groundwater exploration activities. Figure 3b shows a 2-D model of a dolerite intrusion flanked by fracture networks that can serve as pathways for groundwater circulation. The scenario in ERT profile 1 acquired within the north-central (i.e., Amunga) area is analogous to the hypothetical model of the dolerite dyke reported by Senger et al. (2015). The dolerite intrusions in granite gneisses are essential in locating potential aquifers (Molaba 2017). The contact zones may also provide potential groundwater conduits as increased chemical weathering processes due to percolating water is prevalent in such zones. Figure 3c shows a simplified model of the dolerite dyke within Amunga. The flanks of the dyke that show evidence of syn-emplacement fractures (i.e., zones 2 and 3) are likely groundwater targets within the area. Amunga and environs (i.e., Utuhu, Bishiri and Begiaba), which lie within the dolerite intrusive area, may likely have moderate groundwater potential. Beyond the dolerite dyke present in this area, network of fractures are predominant and constitute area of high groundwater potential. Areas where lineaments are concentrated can provide good groundwater prospects (Fig. 7). VES locations along major fracture zones, which have been filled with colluviums and zone of multiple fracture sets with thickness between 20 and 35 m, are likely to have good groundwater potentials. The electrical resistivity range of within such groundwater conduits is 150–700 Ω m (Table 2).

The high groundwater potential areas include Begiatsul, Lishikwel, Okambi, Busanfong, Karo, Kukare, Kikong and Ashikpe. Locations that are slightly away from major fracture zones, such as Beebong, Bayaga, Kundeve, Belinge and Begiaba, which have probably been subjected to second order fracturing and have fractured aquifer with electrical resistivity and thickness in the ranges $\sim$ 20 to 1200 Ω m and 10–25 m, respectively, may likely possess moderate groundwater prospect. Lastly, a unique hydrogeological situation was observed around Alege along a fault zone. In this area, the fault creates a pathway for water to flow through and saturate the saprolitic material and the saprock which are potential groundwater conduits that underlie the kaolin deposit in the area. The electrical resistivity values increased from low (i.e., $<$ 40 Ω m) within the kaolin dominated layer to relatively high value (i.e., between 470 and 651 Ω m) within the saprolite and saprock layers typical of groundwater saturated areas in hard rock terrains. The groundwater potential within Alege is moderate to good. A conceptual model of the kaolin deposit and its underlying saprolite is shown in Figure 6. Generally, the possible sources of recharge are infiltrations from rivers, rivulets and streams that flow within adjoining areas and principally precipitation.

CONCLUSIONS

ERT and VES techniques were employed to characterize hard rock hydrodynamic systems that can serve as potential pathways and conduits for groundwater circulation within the Obudu Basement Complex. Four ERT profiles and 30 VES investigations were completed during the data acquisition campaign. The advantage of the ERT and VES methods is based on their capacity to resolve geological discontinuities in complex geological environments. The geological data used to constrain the electrical resistivity data during the modeling process include the generalized geological,

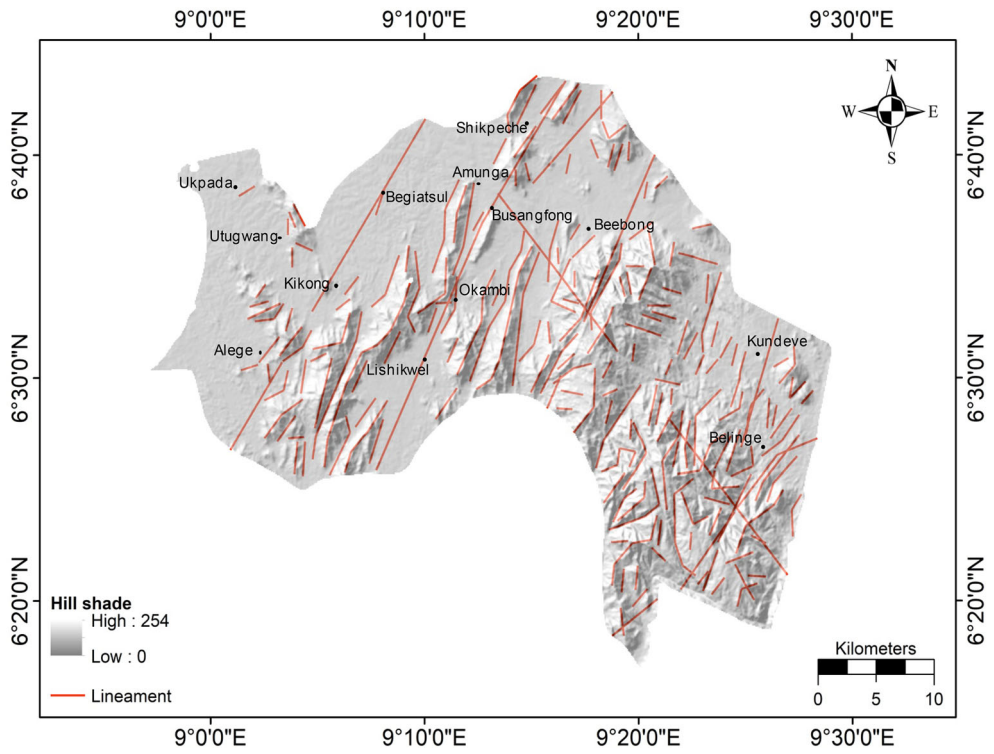

Figure 7. Lineament map of the study area.

Table 2. Summary of lithologic unit types, apparent resistivity ranges and groundwater prospects in Obudu hard rock terrain

S/N	Lithologic unit	Apparent resistivity (Ω m)	Groundwater prospect
1	**Regolith**		
	Dominantly clay (e.g., *kaolinite*)	< 20–100	Poor potential
	Sandy clay	100–150	Moderate potential
	Gravely clay (*Saprolite*)	150–300	Good potential
2	**Fractured bedrock** (*Granite, gneiss, schist, migmatite*)		
	Highly fractured with interconnectivity of fractures	225–700	Good potential
	Moderately fractured with interconnectivity	750–1240	Moderate potential
	Poorly fractured with less interconnectivity	1300–3140	Poor potential
3	**Fresh basement** (*Granite, gneiss, schist, migmatite*)	> 3140	Practically impermeable
	Little or no fractures and no interconnectivity		

borehole lithologic log, kaolin mine pit walls and tectonic information of the area. The rocks are predominantly gneisses, which, in several locations especially the western portion of the study area, have been weathered considerably resulting in thick regolith layers. Three potential hydrogeological scenarios were identified from the ERT profiles investigated in the study. These include the regolith-, doleritic- and kaolin-induced groundwater conduits. Within the central portion of the study area, transtensional stress regimes traceable to the neo- and post-Proterozoic orogenic events resulted in strike-slip faults. Several tectonic events also resulted in cataclastic deformation of gneissic rocks creating pathways for groundwater circulation. Additionally, doleritic intrusions cataclastically deformed host rock resulting in syn-emplacement fractures, which created pathways for groundwater

flow. The multiple fractures and increased fracture density resulting from paleo-thermo-tectonic events may increase the hydrodynamic conditions within the north-central region of the study area. Reduced apparent electrical resistivity around Amunga and environs where doleritic rocks are prevalent is indicative of cataclastic deformation, which allows meteoric fluid such as groundwater access to the bedrock, thereby increasing the rate of in situ chemical weathering of the underlying granite gneisses. This is evident in the low resistivity values ($< 200\ \Omega$ m) observed within the area. Table 2 shows a summary of the groundwater potential of some rocks in the area based on the electrical resistivity values. Areas with high lineament density and those located within the major fault lines show moderate to good groundwater potential due to the presence of multiple interconnected fractures. Moreover, streams and rivers within these areas infiltrate through the pathways created by the faults and tend to increase groundwater circulation within the conduits created by cataclastics and their reworked counterparts.

ACKNOWLEDGMENTS

The authors are grateful to the University of Calabar, Calabar-Nigeria that provided the resources used in conducting the research. The contributions of the Editor and anonymous reviewers are greatly acknowledged.

REFERENCES

Adams, S. (2009). Basement aquifers of southern Africa: Overview and research needs. In R. Titus, H. Beekman, S. Adams, & L. Strachan (Eds.), *The basement aquifers of South Africa* (pp. 1–4). WRC Report No. TT 428/09. Pretoria: Water Research Commission.

Akpan, A. E., Ebong, E. D., & Ekwok, S. E. (2015a). Assessment of the state of soils, shallow sediments and groundwater salinity in Abi, Cross River State, Nigeria. *Environmental Earth Sciences, 73*(12), 8547–8563.

Akpan, A. E., Ebong, E. D., & Emeka, C. N. (2015b). Exploratory assessment of groundwater vulnerability to pollution in Abi, southeastern Nigeria, using geophysical and geological techniques. *Environmental Monitoring and Assessment, 187*(4), 156.

Akpan, A. E., Ekwok, S. E., & Ebong, E. D. (2016). Seasonal reversals in groundwater flow direction and its role in the recurrent Agwagune landslide problem: A geophysical and geological appraisal. *Environmental Earth Sciences, 75*(5), 429.

Akpan, A. E., Ekwok, S. E., Ebong, E. D., George, A. M., & Okwueze, E. E. (2018). Coupled geophysical characterization of shallow fluvio-clastic sediments in Agwagune, southeastern Nigeria. *Journal of African Earth Sciences, 143,* 67–78.

Akpan, A. E., Ugbaja, A. N., & George, N. J. (2013). Integrated geophysical, geochemical and hydrogeological investigation of shallow groundwater resources in parts of the Ikom–Mamfe Embayment and the adjoining areas in Cross River State, Nigeria. *Environmental Earth Sciences, 70*(3), 1435–1456.

Almadani, S., Ibrahim, E., Al-Amri, A., Fnais, M., & Abdelrahman, K. (2019). Delineation of a fractured granite aquifer in the Alwadeen area, Southwest Saudi Arabia using a geoelectrical resistivity survey. *Arabian Journal of Geosciences, 12*(15), 449.

Attwa, M., Akca, I., Basokur, A. T., & Günther, T. (2014). Structure-based geoelectrical models derived from genetic algorithms: A case study for hydrogeological investigations along Elbe River coastal area, Germany. *Journal of Applied Geophysics, 103,* 57–70.

Berkowitz, B., & Balberg, I. (1993). Percolation theory and its application to groundwater hydrology. *Water Resources Research, 29*(4), 775–794.

Chilton, P. J., & Foster, S. S. D. (1995). Hydrogeological characterisation and water-supply potential of basement aquifers in tropical Africa. *Hydrogeology Journal, 3*(1), 36–49.

Das, S., & Pardeshi, S. D. (2018). Comparative analysis of lineaments extracted from Cartosat, SRTM and ASTER DEM: A study based on four watersheds in Konkan region, India. *Spatial Information Research, 26*(1), 47–57.

Ebong, E. D., Akpan, A. E., Emeka, C. N., & Urang, J. G. (2017). Groundwater quality assessment using geoelectrical and geochemical approaches: Case study of Abi area, southeastern Nigeria. *Applied Water Science, 7*(5), 2463–2478.

Ebong, E. D., Akpan, A. E., & Onwuegbuche, A. A. (2014). Estimation of geohydraulic parameters from fractured shales and sandstone aquifers of Abi (Nigeria) using electrical resistivity and hydrogeologic measurements. *Journal of African Earth Sciences, 96,* 99–109.

Edem, G. O., Ekwueme, B. N., Ephraim, B. E., & Igonor, E. E. (2016). Preliminary investigation of pegmatites in Obudu Area, Southeastern Nigeria, using stream sediments geochemistry. *Global Journal of Pure and Applied Sciences, 22*(2), 167–175.

Edet, A., & Okereke, C. (2005). Hydrogeological and hydrochemical character of the regolith aquifer, northern Obudu Plateau, southern Nigeria. *Hydrogeology Journal, 13*(2), 391–415.

Edet, A. E., & Okereke, C. S. (1997). Assessment of hydrogeological conditions in basement aquifers of Precambrian Oban massif, southeastern Nigeria. *Journal of Applied Geophysics*, *36*, 195–204.

Ejiogu, B. C., Opara, A. I., Nwosu, E. I., Nwofor, O. K., Onyema, J. C., & Chinaka, J. C. (2019). Estimates of aquifer geo-hydraulic and vulnerability characteristics of Imo State and environs, Southeastern Nigeria, using electrical conductivity data. *Environmental Monitoring and Assessment, 191*(4), 238.

Ekwok, S. E., Akpan, A. E., Kudamnya, E. A., & Ebong, E. D. (2020). Assessment of groundwater potential using geophysical data: A case study in parts of Cross River State, southeastern Nigeria. *Applied Water Science*, *10*(6), 44.

Ekwueme, B. N. (1990). Rb–Sr ages and petrologic features of Precambrian rocks from the Oban Massif, southeastern Nigeria. *Precambrian Research, 47*(3–4), 271–286.

Ekwueme, B. N. (1994). Structural features of southern Obudu Plateau, Bamenda massif, SE Nigeria: Preliminary interpretations. *J. Min. Geol., 30*(1), 45–59.

Ekwueme, B. N. (2003). *The Precambrian geology and evolution of the Southeastern Nigerian Basement Complex*. Calabar: University of Calabar Press.

Fang, Y., & Jawitz, J. W. (2019). The evolution of human population distance to water in the USA from 1790 to 2010. *Nature Communications, 10*(1), 1–8.

Fazzito, S. Y., Rapalini, A. E., Cortés, J. M., & Terrizzano, C. M. (2009). Characterization of quaternary faults by electric resistivity tomography in the Andean Precordillera of Western Argentina. *Journal of South American Earth Sciences, 28*(3), 217–228.

Ganas, A., Pavlides, S., & Karastathis, V. (2005). DEM-based morphometry of range-front escarpments in Attica, central Greece, and its relation to fault slip rates. *Geomorphology, 65*(3–4), 301–319.

Gélis, C., Revil, A., Cushing, M. E., Jougnot, D., Lemeille, F., Cabrera, J., & Rocher, M. (2010). Potential of electrical resistivity tomography to detect fault zones in limestone and argillaceous formations in the experimental platform of Tournemire, France. *Pure and Applied Geophysics, 167*(11), 1405–1418.

George, N. J., Ibanga, J. I., & Ubom, A. I. (2015). Geoelectro-hydrogeological indices of evidence of ingress of saline water into freshwater in parts of coastal aquifers of Ikot Abasi, southern Nigeria. *Journal of African Earth Sciences, 109,* 37–46.

Gustafson, G. U. N. N. A. R., & Krásný, J. (1994). Crystalline rock aquifers: Their occurrence, use and importance. *Applied Hydrogeology, 2*(2), 64–75.

Inoubli, N., Gouasmia, M., Gasmi, M., Mhamdi, A., & Dhia, H. B. (2006). Integration of geological, hydrochemical and geophysical methods for prospecting thermal water resources: The case of the Hmeïma region (Central–Western Tunisia). *Journal of African Earth Sciences, 46*(3), 180–186.

LaBrecque, D. J., Miletto, M., Daily, W., Ramirez, A., & Owen, E. (1996). The effects of noise on Occam's inversion of resistivity tomography data. *Geophysics, 61*(2), 538–548.

Levinson, A. A. (1980). *Exploration geochemistry* (p. 924). Wilmette, IL: Applied Publishing.

Liu, S., Sang, S., Pan, Z., Tian, Z., Yang, H., Hu, Q., et al. (2016). Study of characteristics and formation stages of macroscopic natural fractures in coal seam# 3 for CBM development in the east Qinnan block, Southern Quishui Basin, China. *Journal of Natural Gas Science and Engineering, 34,* 1321–1332.

Loke, M. H. (2004). Tutorial: 2-D and 3-D electrical imaging surveys. *ASEG Extended Abstracts, 2004,* 1.

Loke, M. H., & Barker, R. D. (1996). Rapid least-squares inversion of apparent resistivity pseudosections by a quasi-Newton method 1. *Geophysical Prospecting, 44*(1), 131–152.

MacDonald, A. M., & Davies, J. (2000). A brief review of groundwater for rural water supply in sub-Saharan Africa. British Geological Survey technical report WC/00/33.

Mao, H., Zhao, Z., Cui, L., & Liu, C. (2018). The influence of climate and topography on chemical weathering of granitic regoliths in the monsoon region of China. *Acta Geochimica, 37*(5), 758–768.

Molaba, G. L. (2017). *Investigating the possibility of targeting major dolerite intrusives to supplement municipal water supply in Bloemfontein: A geophysical approach* (Doctoral dissertation, University of the Free State).

Ndubueze, D. N., Igboekwe, M. U., & Ebong, E. D. (2019). Assessment of groundwater potential in Ehime Mbano, Southeastern Nigeria. *Journal of Geosciences, 7*(3), 134–144.

Obianwu, V. I., Egor, A. O., Okiwelu, A. A., & Ebong, E. D. (2015). Integrated geophysical studies over parts of Central Cross River State for the determination of groundwater potential and foundation properties of rocks. *Journal of Applied Geology and Geophysics, 3,* 49–64.

O'Connor, G. A., Elliott, H. A., & Bastian, R. K. (2008). Degraded water reuse: An overview. *Journal of Environmental Quality, 37*(S5), S-157.

Oden, M. I., Okpamu, T. A., & Amah, E. A. (2012). Comparative analysis of fracture lineaments in Oban and Obudu Areas, SE Nigeria. *Journal of Geography and Geology, 4*(2), 36.

Odeyemi, I. (1981). A review of the orogenic events in the Precambrian basement of Nigeria, West Africa. *Geologische Rundschau, 70*(3), 897–909.

Okwueze, E. E. (1996). Preliminary findings of the groundwater resource potentials from a regional geo-electric survey of the Obudu basement area. *Nigeria Global Journal of Pure and Applied sciences, 2*(2), 201–211.

Orlović, M., & Krajnović, A. (2015, October). Water management-an important challenge for modern economics. In *DIEM: Dubrovnik international economic meeting* (Vol. 2, No. 1, pp. 487–510). Sveučilište u Dubrovniku.

Peinado-Guevara, H. J., Delgado-Rodríguez, O., Herrera-Barrientos, J., Peinado-Guevara, V. M., Herrera-Barrientos, F., & Leon, S. C. (2017). Determining water salinity in a shallow aquifer and its vulnerability to coastline erosion. *Polish Journal of Environmental Studies, 26*(5), 2001.

Robert, T., Dassargues, A., Brouyère, S., Kaufmann, O., Hallet, V., & Nguyen, F. (2011). Assessing the contribution of electrical resistivity tomography (ERT) and self-potential (SP) methods for a water well drilling program in fractured/karstified limestones. *Journal of Applied Geophysics, 75*(1), 42–53.

Runkel, A. C., Tipping, R. G., Alexander, E. C., Jr., & Alexander, S. C. (2006). Hydrostratigraphic characterization of intergranular and secondary porosity in part of the Cambrian sandstone aquifer system of the cratonic interior of North America: Improving predictability of hydrogeologic properties. *Sedimentary Geology, 184*(3–4), 281–304.

Samsudin, A. R., Haryono, A., Hamzah, U., & Rafek, A. G. (2008). Salinity mapping of coastal groundwater aquifers using hydrogeochemical and geophysical methods: A case study from north Kelantan, Malaysia. *Environmental Geology, 55*(8), 1737–1743.

Sasaki, Y. (1992). Resolution of resistivity tomography inferred from numerical simulation 1. *Geophysical Prospecting, 40*(4), 453–463.

Satpathy, B. N., & Kanungo, D. N. (1976). Groundwater exploration in hard-rock terrain—A case history. *Geophysical Prospecting, 24*(4), 725–736.

Scapozza, C., & Laigre, L. (2014). The contribution of electrical resistivity tomography (ERT) in Alpine dynamics geomorphology: Case studies from the Swiss Alps. *Géomorphologie: Relief, Processus, Environnement, 20*(1), 27–42.

Senger, K., Buckley, S. J., Chevallier, L., Fagereng, Å., Galland, O., Kurz, T. H., et al. (2015). Fracturing of doleritic intrusions and associated contact zones: Implications for fluid flow in volcanic basins. *Journal of African Earth Sciences, 102,* 70–85.

Singhal, B. B. S., & Gupta, R. P. (1999). Fractures and discontinuities. In B. B. S. Singhal & R. P. Gupta (Eds.), *Applied hydrogeology of fractured rocks* (pp. 13–35). Dordrecht: Springer.

Suzuki, K., Toda, S., Kusunoki, K., Fujimitsu, Y., Mogi, T., & Jomori, A. (2000). Case studies of electrical and electromagnetic methods applied to mapping active faults beneath the thick quaternary. In Y. Kanaori, K. Tanaka, & M. Chigira (Eds.), *Developments in geotechnical engineering* (Vol. 84, pp. 29–45). Amstredam: Elsevier.

Titus, R., Witthüser, K., & Walters, B. (2009). Groundwater and mining in the Bushveld Complex. In *Proceedings of the international mine water conference, Pretoria, South Africa* (pp. 178–184).

Uhlemann, S., Chambers, J., Falck, W. E., Tirado Alonso, A., Fernández González, J. L., & Espín de Gea, A. (2018).

Applying electrical resistivity tomography in ornamental stone mining: Challenges and solutions. *Minerals, 8*(11), 491.

Ukwang, E. E., Ekwueme, B. N., & Horsley, R. J. (2003). Petrology of granulite facies rocks in Ukwortung area of obudu plateau, Southeastern Nigeria. *Global Journal of Geological Sciences, 1*(2), 159–168.

Vander Velpen, B. P. A., & Sporry, R. J. (1993). RESIST. A computer program to process resistivity sounding data on PC compatibles. *Computers & Geosciences, 19*(5), 691–703.

Wilkinson, P. B., Meldrum, P. I., Kuras, O., Chambers, J. E., Holyoake, S. J., & Ogilvy, R. D. (2010). High-resolution electrical resistivity tomography monitoring of a tracer test in a confined aquifer. *Journal of Applied Geophysics, 70*(4), 268–276.

Wright, E. P. (1992). The hydrogeology of crystalline basement aquifers in Africa. *Geological Society, London, Special Publications, 66*(1), 1–27.

Yadav, G. S., & Singh, S. K. (2007). Integrated resistivity surveys for delineation of fractures for ground water exploration in hard rock areas. *Journal of Applied Geophysics, 62*(3), 301–312.